International Journal of Science and Research (IJSR)
ISSN: 2319-7064
Impact Factor 2025: 7.089

Study on Molecular Electrostatic Potential, HOMO-LUMO and Chemical Reactivity of Lithium, Sodium and Potassium Salt of Sarcosine by DFT Method

Mahendra B. Dhande

Department of Chemistry, HPT Arts and RYK Science College, Nashik-422005, India
Email: *mbdhande[at]hptrykcollege.com*

Abstract: ***Alkali metals salt of amino acids, due to their large numbers of advantages, are think about as an attractive replacement for alkanolamine solvents for post-combustion CO_2 (main greenhouse gas) removal from combustion products. For designing gas-liquid contactors, process modelling, and working of the equipment for a particular absorbent, its various properties are needed. In the study, using Gaussian 09 software the HOMO/LUMO band gap energy, Molecular Electrostatic Potential, Optimized parameters like total dipole moment, C=O vibration of COOH group, bond lengths, bond angles and Global Reactivity Descriptors of Lithium, Sodium and Potassium Salt of Sarcosine. Study shows that the energy bandgap for potassium salts is less than that of corresponding sodium salts. From result it could be expressed that the change of alkali metal (Li/Na/ K) in amino acid salts are changing the physical structural and chemical activity of amino acid salts. This study would be helpful for their applications as a promising solvent for the removal of CO_2 from flue gases from the combustion.***

Keywords: Amino acid salts, Sarcosine salts, Carbon dioxide removal, Molecular Properties, Alkali metals

1. Introduction

Global warming is the most serious environmental issue threatening the entire world. It is the concerns for corresponding climate change and its potential impact on human kind. Excess CO_2 (carbon dioxide) emissions by a number of sources, involves the burning of fossil fuels to produce energy as well as various industrial and human activities, is the primary contributor to global warming[1,2].

Hence, in numerous CO_2 producing sectors, the removal of CO_2 from a process gas stream becomes a crucial step and may be necessary for operational, financial, and/or environmental reasons. Technologies for CO_2 capture include methods for removing CO_2 from flue gas before the flue gas is released into the atmosphere.

Alkanolamines related absorbents are widely used in such procedures[3]. Alkanolamines degrades in oxygen-rich environments, producing very hazardous degradation compounds[4]. These drawbacks of amine-based solvents limit their application in CO_2 removal procedures.

Alkali salts of amino acids have been found to be potential substitutes for alkanolamine, and numerous studies have demonstrated their interaction with CO_2[5,6]. Amino acids behave similarly to amines and contain the same functional group, which makes them effective CO_2 capture agents. However, there are a number of advantages to using amino acids in this capacity. Besides being more expensive than alkanolamines, amino acids have several special benefits, such as greater stability against oxidative degradation[7], minimal volatility, increased surface tension, and rapid absorption rates[8].

For designing gas–liquid contactors, process modelling, and working of the equipments for a particular absorbent, its physical properties, HOMO/LUMO band gap energy, Molecular Electrostatic Potential, Optimized parameters could be advantageous for their evaluation as a CO_2 absorbing agent and for their other Industrial application. These parameters are also essential for projecting chemical reaction kinetics from CO_2 absorption rate tests[9].

By employing this technique such data for Lithium, Sodium and Potassium salt of Sarcosine have not yet been described in the open literature. Hence, in this studies, using Gaussian 09 software the novel theoretical data like HOMO/LUMO band gap energy, Molecular Electrostatic Potential, Optimized parameters like total dipole moment, bond lengths, bond angles and Global Reactivity Descriptors of Lithium, Sodium and Potassium salt of Sarcosine is presented.

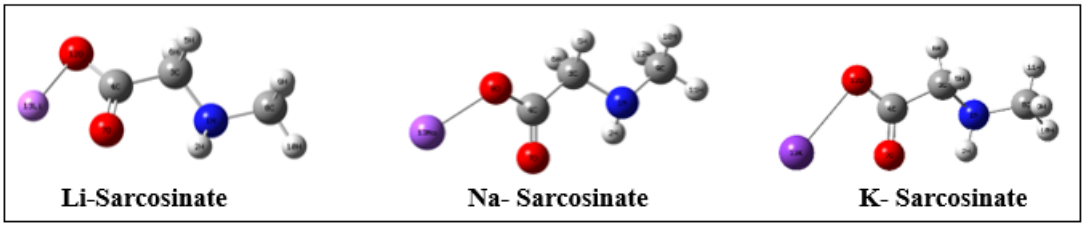

Figure 1: Optimized Geometrical Structures of Li, Na and K-Sarcosinate

2. Materials and Method

Gaussian 09 Software was used for computational work. In the present work HOMO/LUMO band gap energy, Molecular Electrostatic Potential (MEP), Optimized parameters like total dipole moment, bond lengths, bond angles and Global Reactivity Descriptors of Lithium, Sodium and Potassium salt of Sarcosine and other optimized parameters were calculated by using Density Functional Theory (DFT) B3LYP method at 6-31++G (d, p) basis set.[10]

3. Result and Discussion

1) Optimized geometrical parameters (bond length L_{O-M} and bond angle O=C-O)

The optimized geometrical parameters such as bond length L_{O-M} and bond angle O-C=O of –COOM group (M=Li/Na/k) were computed[11] for Li, Na and K-sarcosinate and are placed in Table 1. The O-M bond length and O-C=O bond angle increases from Li to K as the size of Metal-ion increases. Figure 1 presents the optimized geometrical structures for Li, Na and K-Sarcosinate.

Table 1: Optimized geometrical parameters:

Optimized Parameters	Li-Sarcosinate	Na-Sarcosinate	K-Sarcosinate
L_{O-M}	1.86	2.2	2.55
O=C-O	121.18	123.68	124.69

2) Global Molecular Reactivity Descriptors

The eigenvalues of the highest-occupied molecular orbitals (HOMO), lowest-unoccupied molecular orbitals(LUMO), the HOMO-LUMO gap, electronegativity, and chemical hardness are the most well-known of these parameters (Global Reactivity Descriptors) that are based on the DFT[12,13]. The 1930s-era Koopmans theorem[14] provides a different method for predicting the ionization energy and electron affinities of chemical species and serves as a link between conceptual density functional theory and molecular orbital theory. The hardness(ɳ), chemical potential (μ) and electronegativity(χ) and softness (S) are defined on the basis of HOMO and LUMO energy values, for closed-shell molecules using Koopmans's theorem[14,15].

All the calculated values of ionization potential, electron affinity, hardness, softness, potential, and electronegativity for Li, Na and K-sarcosinate are presented in Table 2. The stability of the molecule can also be related to hardness and softness[16]. The chemical hardness value decreases from Li-salt to K-salt as the size of metal ion increases indicating K-salt as most stable salt. It was found lowest electronegativity (χ) values of K-sarcosinate.

Table 2: Molecular properties (Molecular Reactivity Descriptors) including chemical hardness (ɳ), softness (S), chemical potential (μ) and electronegativity (χ)

Molecular properties	Li-Sarcosinate	Na-Sarcosinate	K-Sarcosinate
I	5.8527	5.5376	5.2758
A	1.0844	1.5837	1.3998
Chemical hardness (ɳ)	2.3841	1.9769	1.938
Softness (S)	0.4194	0.5058	0.516
Chemical potential (μ)	-3.4685	-3.5606	-3.3378
Electronegativity (χ)	3.4685	3.5606	3.3378

3) Calculated physical parameters for studied SAA molecules including total dipole moment (TDM), HOMO/LUMO band gap energy (ΔE)

The Total Dipole Moment (TDM) values and HOMO/LUMO band gap energy(ΔE) were also computed and compiled in Table 3. The two physical parameters TDM and ΔE measures the reactivity [17,18] and stabilty[19] of a given compound with their surrounding molecules. High total dipole moment and a low band gap energy is an indication of reactive compounds[20]. TDM is increased and band gap energy slightly decreased from Li-sarcocinate to Na- sarcocinate and from Na-sarcocinate to K- sarcocinate.

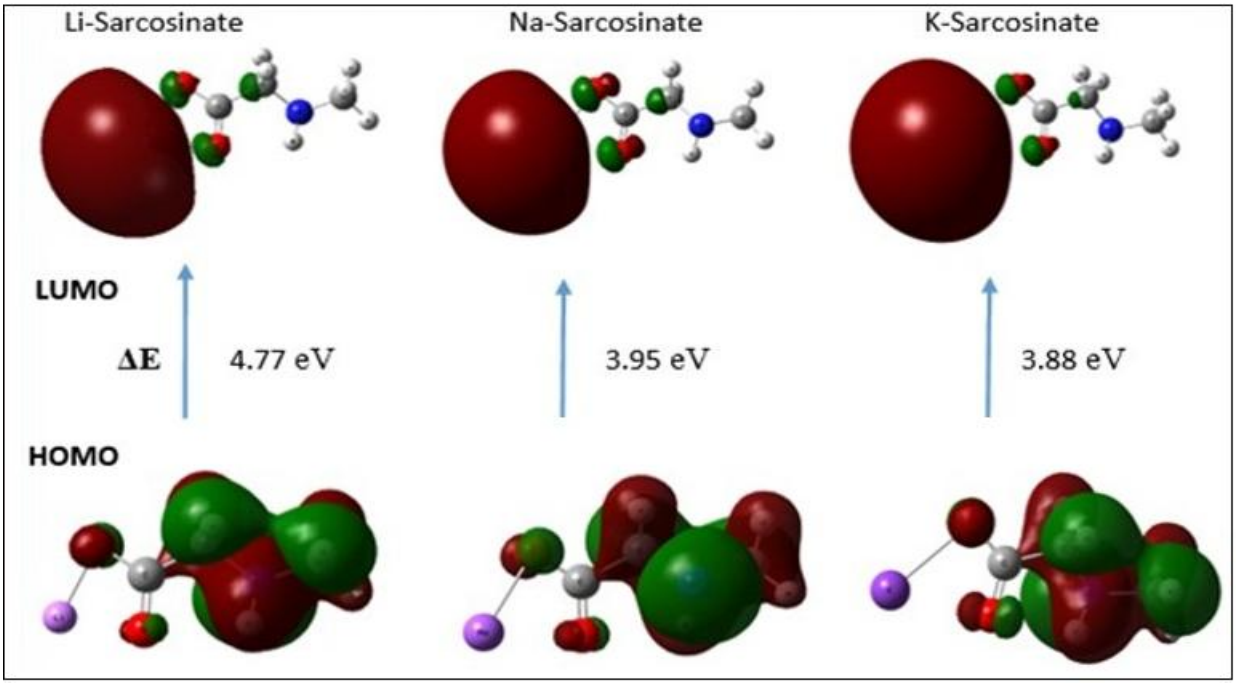

Figure 2: FMO Diagrams of Li, Na and K- Sarcosinate

Table 3: Total dipole moment (TDM) and HOMO/LUMO band gap energy (ΔE)

Physical parameters	Li-Sarcosinate	Na-Sarcosinate	K-Sarcosinate
Total Dipole Moment (TDM) D	3.87	6.25	8.32
HOMO E (eV)	-5.85	-5.54	-5.28
LUMO E (eV)	-1.08	-1.58	-1.4
ΔE (eV)	4.77	3.95	3.88

4) Molecular Electrostatic Potential (MEP) Map Analysis

The MEP map is one of the key tool for predicting the electrophilic (negative potential) and nucleophilic (positive potential) areas of organic or inorganic compounds. In other words, it is a rather accurate charge density estimator[21]. Additionally, it offers data on hydrogen bond interactions, chemical reactions, and biological activity prediction. The following color scale defines the magnitude of the electrostatic potential: red < orange < yellow < green < cyan < blue[22]. In this color scheme, negative, slightly electron-rich, zero potential, and positive regions are represented by the colors red, yellow, green, and blue, respectively[23].

The molecular electrostatic potential (MEP) is used to predict the relative activity positions in a species for a nucleophilic or electrophilic attack. The optimized structure using B3LYP/6-31G*(d,p) basic set was used in the DFT calculation to determine the MEP surface analysis of the salt molecules. Figure 3 shows the electrostatic potential surface map of the investigated Li, Na and K-Sarcosinate.

In the MEP structure, the colors red and blue indicate more electron-rich and electron-poor regions, respectively. The chemical clearly exhibits the polarization effect. The positive potential regions are located over the hydrogen atoms in the MEP, while the negative potential regions are located over the electro-negative atoms (oxygen, and nitrogen). Consequently, locations with more negative electronegative potential and positive electrostatic potential are more conducive to attracting nucleophilic and electrophilic molecules.

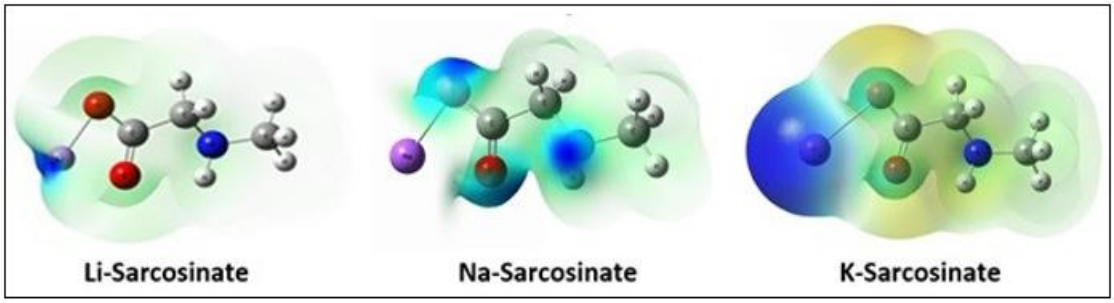

Figure 3: Molecular Electrostatic Potential (MEP) of Li, Na and K- Sarcosinate

5) Mullikan's Atomic Charges (Population Analysis) of Li, Na and K-Sarcosinate.

Density Functional Theory (DFT) B3LYP method at 6-31++G (d, p) basis set was used to calculate the Mulliken atomic charges of the optimized crystal structure. The Mulliken atomic charge distribution is listed in Table 4. The Mulliken atomic charges on carbon atoms were shown to be either positive or negative. Due to the presence of an electronegative atom (N1), H2 obtained a greater positive charge than the other hydrogen atoms, yet all hydrogen atoms were shown to have a positive charge. They function as acceptor atoms. It was found highest positive charge on H2 of Na-Sarcosinate among all studied salts. Additionally, all of the optimized compound's oxygen atoms were found to have a negative charge, which functions as donor atoms.

Table 4: Mullikan's Atomic Charges of Li, Na and K-Sarcosinate.

S. No	Atom	Charge		
		Li-Sarcosinate	Na-Sarcosinate	K-Sarcosinate
1	N1	-0.29499	-0.29552	-0.28962
2	H2	0.31494	0.315391	0.306589
3	C3	-0.43456	-0.50691	-0.43315
4	C4	0.61492	0.511417	0.518399
5	H5	0.193886	0.190261	0.188666
6	H6	0.150334	0.146312	0.144282
7	O7	-0.58934	-0.66901	-0.65073
8	O8	-0.55711	-0.61839	-0.62009
9	C9	-0.37676	-0.37531	-0.36974
10	H10	0.148564	0.14718	0.149081
11	H11	0.128326	0.12764	0.126544
12	H12	0.154039	0.15361	0.153557
13	M13= Li/Na/K	0.547741	0.873329	0.776214

Acknowledgement

Authors thanks Dr. Krishna Chaitanya G. SRTMU, Nanded for providing Computational lab for carrying out computational work and Principal, HPT Arts and RYK Science College, Nashik, India.

References

[1] Alcalde J, Flude S, Wilkinson M, Johnson G, Edlmann K, Bond CE, Scott V, Gilfillan SM, Ogaya X, Haszeldine RS. Estimating geological CO2 storage security to deliver on climate mitigation. Nature communications. 2018 Jun 12;9(1):2201.

[2] Olivier JG, Peters JA. Trends in global CO2 and total greenhouse gas emissions: 2020 report. PBL Netherlands Environmental Assessment Agency, The Hague. 2020 [Internet]. 2020

[3] Ping T, Dong Y, Shen S. Energy-efficient CO2 capture using nonaqueous absorbents of secondary alkanolamines with a 2-butoxyethanol cosolvent. ACS Sustainable Chemistry & Engineering. 2020 Nov 28;8(49):18071-82.

[4] Vitillo JG, Smit B, Gagliardi L. Introduction: carbon capture and separation. Chemical reviews. 2017 Jul 26;117(14):9521-3.

[5] Liu M, Gadikota G. Single-step, low temperature and integrated CO2 capture and conversion using sodium glycinate to produce calcium carbonate. Fuel. 2020 Sep 1; 275: 117887.
[6] Xu, X.; Myers, M. B.; Versteeg, F. G.; Adam, E.; White, C.; Crooke, E.; Wood, C. D. *Journal of Materials Chemistry A*, **9(3)**, 1692-1704 (2021).
[7] Chang YT, Leron RB, Li MH. Carbon dioxide solubility in aqueous potassium salt solutions of l-proline and dl-α-aminobutyric acid at high pressures. The Journal of Chemical Thermodynamics. 2015 Apr 1; 83: 110-6.
[8] Garcia AA, Leron RB, Soriano AN, Li MH. Thermophysical property characterization of aqueous amino acid salt solutions containing α-aminobutyric acid. The Journal of Chemical Thermodynamics. 2015 Feb 1; 81: 136-42.
[9] Li H, Guo H, Shen S. Water-lean blend mixtures of amino acid salts and 2-methoxyethanol for CO2 capture: Density, viscosity and solubility of CO2. The Journal of Chemical Thermodynamics. 2020 Nov 1; 150: 106237.
[10] M. J. Frisch, G. W. Trucks, H. B. Schlegel, G. E. Scuseria, M. A. Robb, J. R. Cheeseman, G. Scalmani, V. Barone, B. Mennucci, G. A. Petersson, H. Nakatsuji, M. Caricato, X. Li, H. P. Hratchian, A. F. Izmaylov, J. Bloino, G. Zheng, J. L. Sonnenberg, M. Hada, M. Ehara, K. Toyota, R. Fukuda, J. Hasegawa, M. Ishida, T. Nakajima, Y. Honda, O. Kitao, H. Nakai, T. Vreven, J. A. Montgomery, Jr., J. E. Peralta, F. Ogliaro, M. Bearpark, J. J. Heyd, E. Brothers, K. N. Kudin, V. N. Staroverov, T. Keith, R. Kobayashi, J. Normand, K. Raghavachari, A. Rendell, J. C. Burant, S. S. Iyengar, J. Tomasi, M. Cossi, N. Rega, J. M. Millam, M. Klene, J. E. Knox, J. B. Cross, V. Bakken, C. Adamo, J. Jaramillo, R. Gomperts, R. E. Stratmann, O. Yazyev, A. J. Austin, R. Cammi, C. Pomelli, J. W. Ochterski, R. L. Martin, K. Morokuma, V. G. Zakrzewski, G. A. Voth, P. Salvador, J. J. Dannenberg, S. Dapprich, A. D. Daniels, O. Farkas, J. B. Foresman, J. V. Ortiz, J. Cioslowski, D. J. Fox, Gaussian. **2013,** Inc., Wallingford CT.
[11] Tayade K, Bondhopadhyay B, Basu A, Chaitanya GK, Sahoo SK, Singh N, Attarde S, Kuwar A. A novel urea-linked dipodal naphthalene-based fluorescent sensor for Hg (II) and its application in live cell imaging. Talanta. 2014 May 1;122:16-22.
[12] Kaya S, Tüzün B, Kaya C, Obot IB. Determination of corrosion inhibition effects of amino acids: quantum chemical and molecular dynamic simulation study. Journal of the Taiwan Institute of Chemical Engineers. 2016 Jan 1; 58: 528-35.
[13] Valaboju A, Gunturu KC, Kotamarthi B, Joly D, Hissler M. DFT study of Host-Dopant systems of DPVBi with Organophosphorus π-Conjugated materials. Computational and Theoretical Chemistry. 2017 Aug 1; 1113: 61-71.
[14] Koopmans T. Ordering of wave functions and eigenenergies to the individual electrons of an atom. Physica. 1933; 1: 104-13.
[15] Pearson RG. Chemical hardness and density functional theory. Journal of Chemical Sciences. 2005 Sep; 117(5): 369-77.
[16] Dheivamalar S, Banu KB. A DFT study on functionalization of acrolein on Ni-doped (ZnO) 6 nanocluster in dye-sensitized solar cells. Heliyon. 2019 Dec 1;5(12).
[17] Ibrahim M, Mahmoud AA. Computational notes on the reactivity of some functional groups. Journal of Computational and Theoretical Nanoscience. 2009 Jul 1;6(7):1523-6.
[18] Ezzat HA, Hegazy MA, Nada NA, Ibrahim MA. Effect of nano metal oxides on the electronic properties of cellulose, chitosan and sodium alginate. Biointerface Res. Appl. Chem. 2019;9(4):4143-9.
[19] Singh JS. IR and Raman spectra with Gaussian-09 molecular analysis of some other parameters and vibrational spectra of 5-fluoro-uracil: JS Singh. Research on Chemical Intermediates. 2020 May;46(5):2457-79.
[20] Miar, M., 2021. Shiroudi A. Pourshamsian K. Oliaey AR Hatamjafari F. Theoretical investigations on the HOMO–LUMO gap and global reactivity descriptor studies, natural bond orbital, and nucleus-independent chemical shifts analyses of 3-phenylbenzo [d] thiazole-2 (3 H)-imine and its para-substituted derivatives: Solvent and substituent effects. *J. Chem. Res*, *45*(1-2), pp.147-158.
[21] F. Boursas, F. Berrah, N. Kanagathara, G. Anbalagan, S. Bouacida, Xrd, ft-ir,, FT Raman spectra and ab initio HF vibrational analysis of bis (5-amino-3- carboxy- 1H-1,2,4-triazol-4-ium) selenate dehydrate, J. Mol. Struct. 1180 (2019) 532e541.
[22] K. Sharma, R. Melavanki, S.S. Patil, R. Kusanur, N.R. Patil, V.M. Shelar, Spectroscopic behavior, FMO, NLO and NBO analysis of two novel aryl boronic acid derivatives: experimental and theoretical insights, J. Mol. Struct. 1181 (2019) 474e487.
[23] S. Xavier, S. Periandy, K. Carthigayan, S. Sebastian, Molecular docking, TG/DTA, molecular structure, harmonic vibrational frequencies, natural bond orbital and TD-DFT analysis of diphenyl carbonate by DFT approach, J. Mol. Struc. 1125 (2016) 204–216.